

Detonation Performance and Shock Sensitivity of Energetic Material NTO with Embedded Small Molecules: Deep Neural Network Potential Accelerated Molecular Dynamics Study

Caimu Wang,^{1,2} Jidong Zhang,³ Wei Guo,^{*,1,2} Ruibin Liu,^{1,2} and Yugui Yao^{1,2}

¹ *Frontiers Science Center for High Energy Material (MOE), Beijing Institute of Technology, Beijing 100081, China*

² *Centre for Quantum Physics, Key Laboratory of Advanced Optoelectronic Quantum Architecture and Measurement (MOE), School of Physics, Beijing Institute of Technology, Beijing 100081, China*

³ *Department of Physics, College of Science, Shihezi University, Shihezi 832003, China*

Supplementary Information

Table S1. Comparison of NTO crystal density calculated at 0 K with various methods describing van der Waals interactions and experimental result.

Methods	Density (g/cm ³)	Relative error (%)
DFT-D3	1.901	1.30
DFT-D2	1.895	1.61
DFT-Tkatchenko-Scheffler	1.882	2.28
DFT-ulg	1.857	3.58
DFT without vdW	1.702	11.63
Experiment	1.926	—

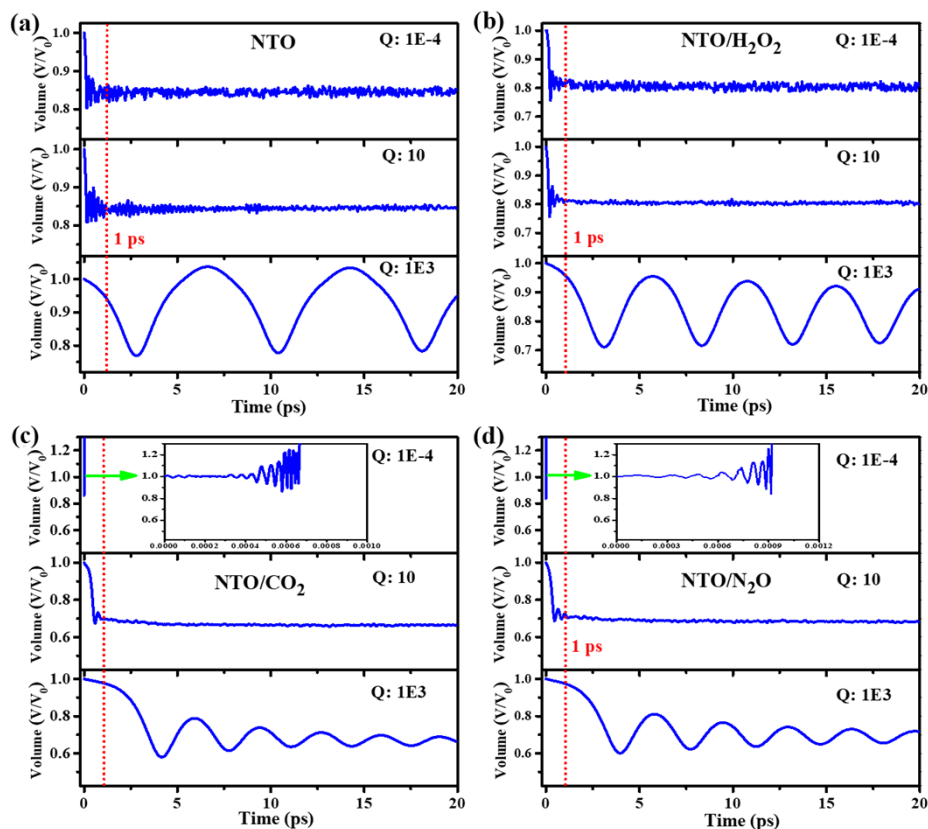


Figure S1. The evolution of relative volume under MSST-MD simulations at the shock velocity of 5.0 km/s with different cell mass-like parameters and zero artificial viscosity for (a) NTO, (b) NTO/H₂O₂, (c) NTO/CO₂, and (d) NTO/N₂O system. The red lines represent the moment of 1 ps. The unit of mass-like Q is 10^{-13} kg²/m⁴. Selecting an excessively large Q (1E3) can lead to long-lived oscillations, whereas too small Q (1E-4) can cause large amplitude oscillations that do not decay with time in the NTO and NTO/H₂O₂ system. An excessively small value of Q (1E-4) induces large amplitude oscillations around the initial volume and causes the program to fail in the NTO/CO₂ and NTO/N₂O system. This phenomenon reveals that too small Q may lead to instability in the MSST simulation.

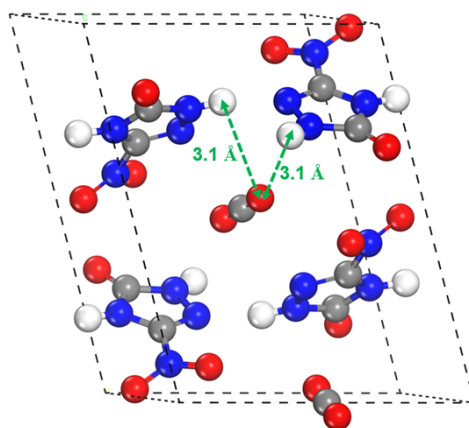


Figure S2. Structure of the NTO/CO₂ crystal. The C, H, O, and N atoms are gray, white, red, and blue, respectively. Bond lengths are labeled with green dotted lines in the figure.

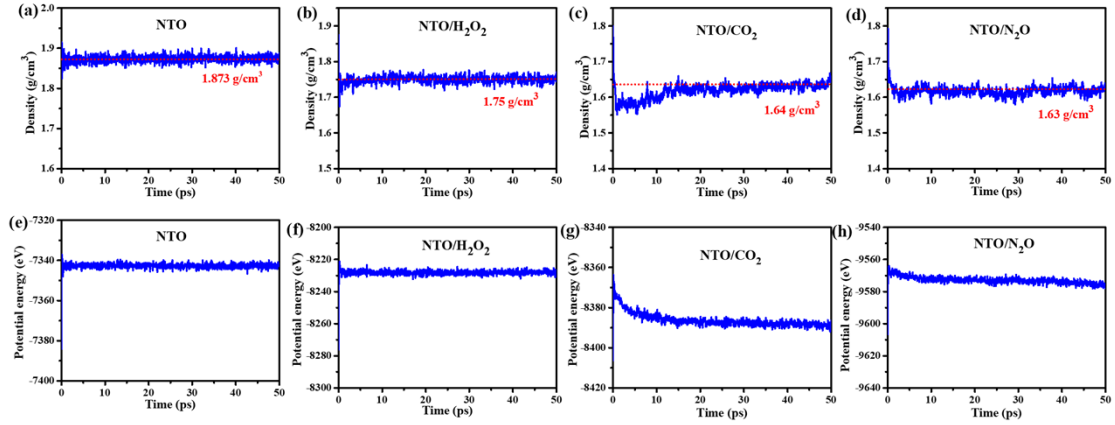


Figure S3. Evolution of (a)-(d) crystal densities and (e)-(h) potential energies for $3 \times 4 \times 2$ supercell of the four systems under NPT-MD simulations at ambient conditions. The red dotted lines represent the average densities of systems for the last 10 ps MD simulations.

Table S2. Surface energies of (1 0 0), (0 1 0) and (0 0 1) surface for NTO/CO₂ and NTO/N₂O system.

The surface energy is defined as follows:

$$\sigma = \frac{1}{2A}(E_{slab} - nE_{mole})$$

Herein, E_{slab} , A , and n represent the total energy, surface area and molecular number of the slab model, respectively, and E_{mole} represents the energy per molecule in bulk crystal.

System	Slab	Surface energy (J/m ²)
NTO/CO ₂	(1 0 0) terminated with NTO	0.18
	(1 0 0) terminated with CO ₂	0.19
	(0 1 0)	0.22
	(0 0 1) terminated with NTO	0.05
	(0 0 1) terminated with CO ₂	0.03
NTO/N ₂ O	(1 0 0) terminated with NTO	0.20
	(1 0 0) terminated with N ₂ O	0.16
	(0 1 0)	0.18
	(0 0 1) terminated with NTO	0.05
	(0 0 1) terminated with N ₂ O	0.03

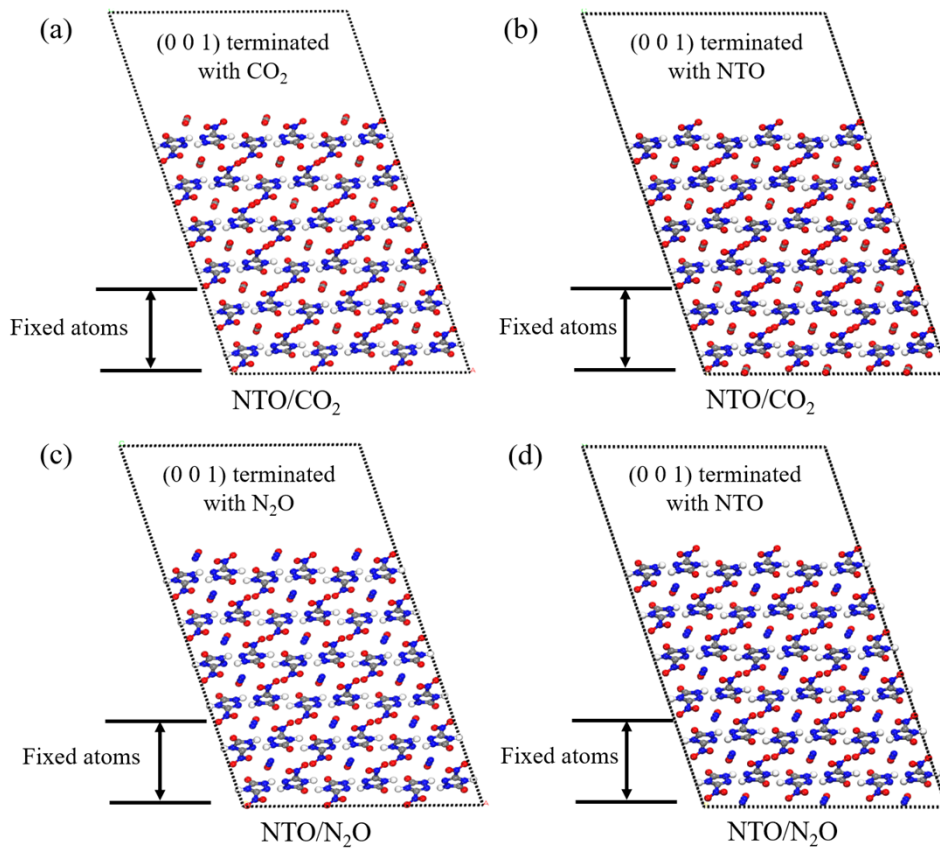


Figure S4. NTO/ CO_2 (0 0 1) slab terminated with (a) CO_2 and (b) NTO molecules. NTO/ N_2O (0 0 1) slab terminated with (c) N_2O and (d) NTO molecules.

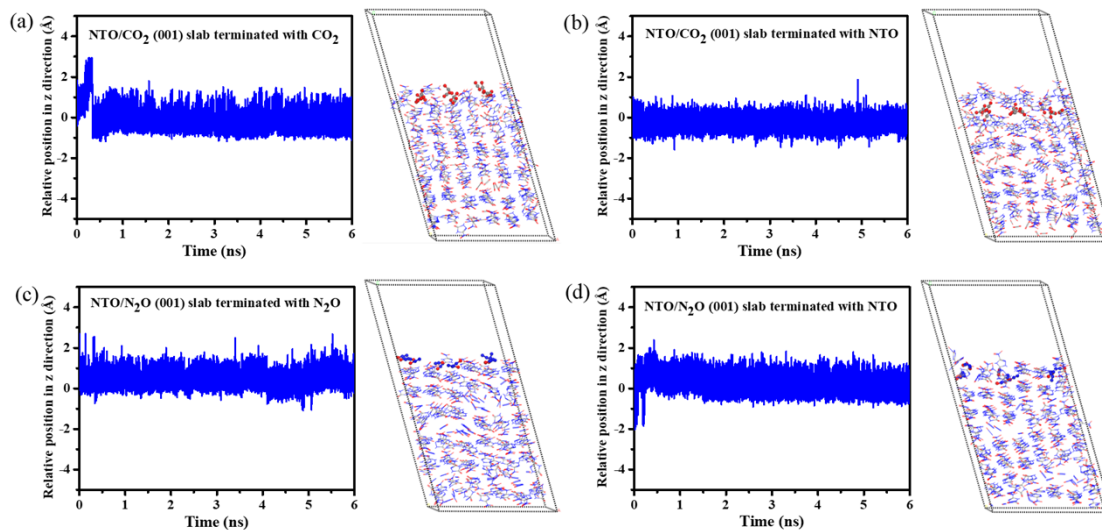


Figure S5. Relative positions in z direction of the top most atoms in the surface $\text{CO}_2/\text{N}_2\text{O}$ molecule. The right insets show the final snapshots in the 6 ns' MD simulations. The $\text{CO}_2/\text{N}_2\text{O}$ molecules at the terminal of the slab are represented with balls. The zero position in z is defined as the initial position of the corresponding atoms.

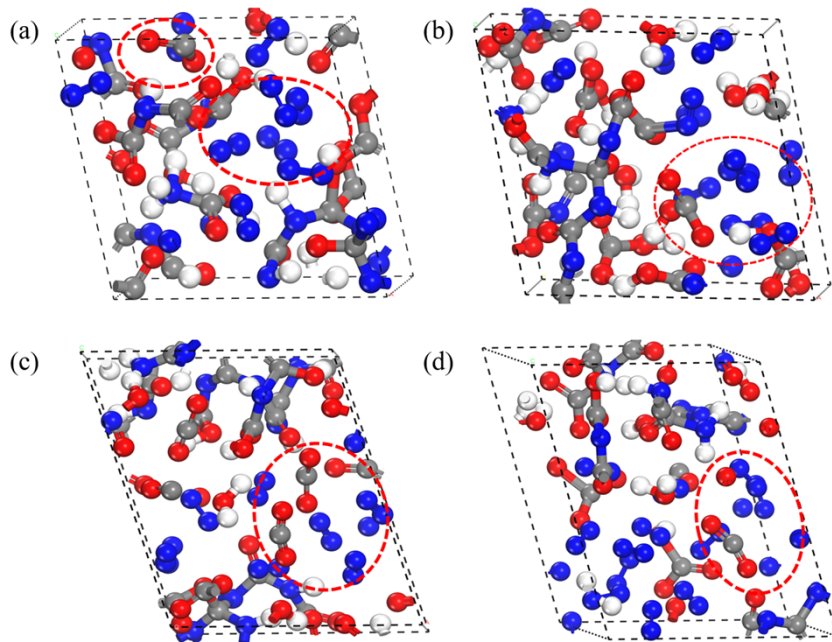


Figure S6. The last configurations of (a) NTO, (b) NTO/H₂O₂, (c) NTO/CO₂, and (d) NTO/N₂O in DNNP-MD simulations lasting for 100 ps. MD simulations are performed at 3000 K, and the volume of the system was initially compressed to 65% of its original volume. Stable N₂ and CO₂ molecules are generated in MD simulations, as shown in the red circles.

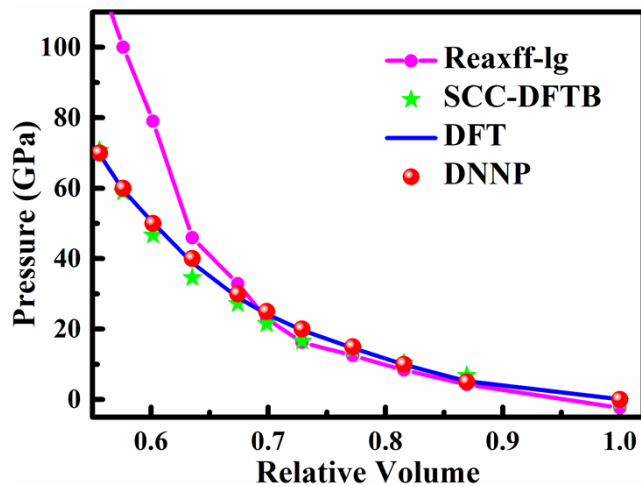


Figure S7. Comparison of the relative volume of NTO crystals versus the external pressure calculated by DNNP, DFT, SCC-DFTB, and the Reaxff-1g method.

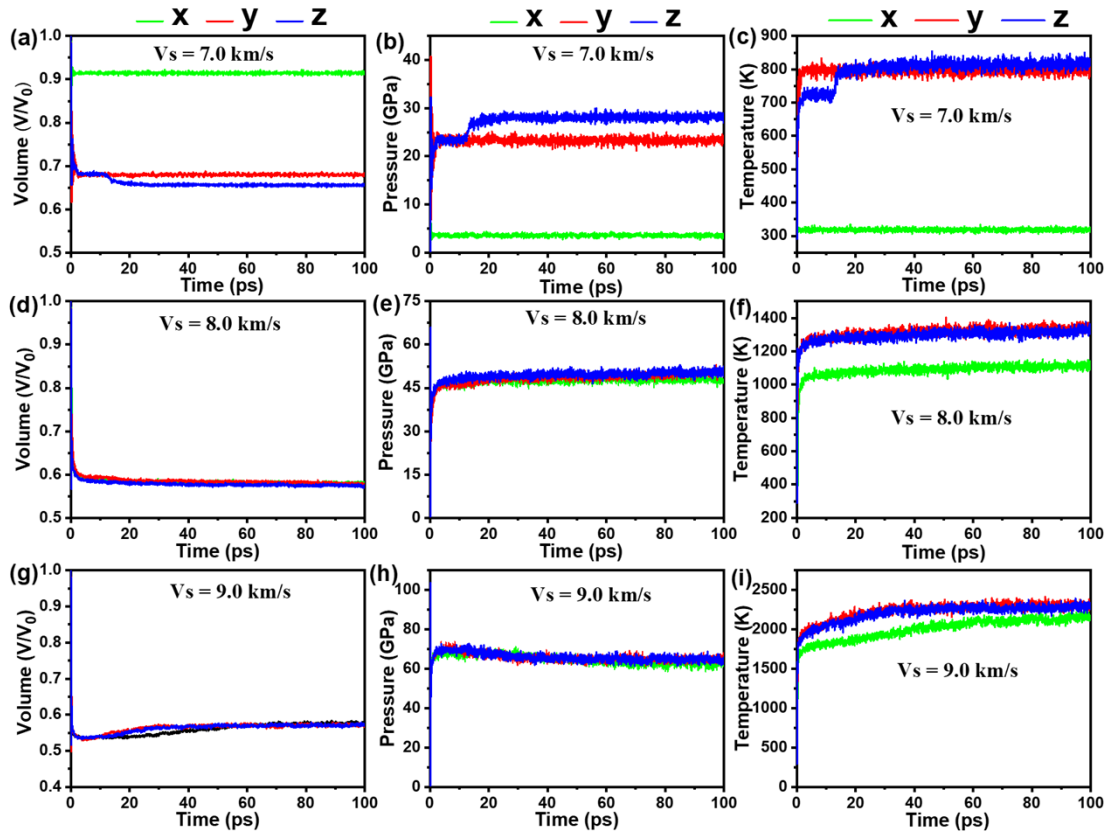


Figure S8. The shock response of NTO. (a)-(c) are the evolution of volume, pressure, and temperature for a low-strength shock speed of 7.0 km/s. (d)-(f) are the evolution of volume, pressure, and temperature for a shock speed of 8.0 km/s. (g)-(h) are the evolution of volume, pressure, and temperature for a high strength shock speed of 9.0 km/s.

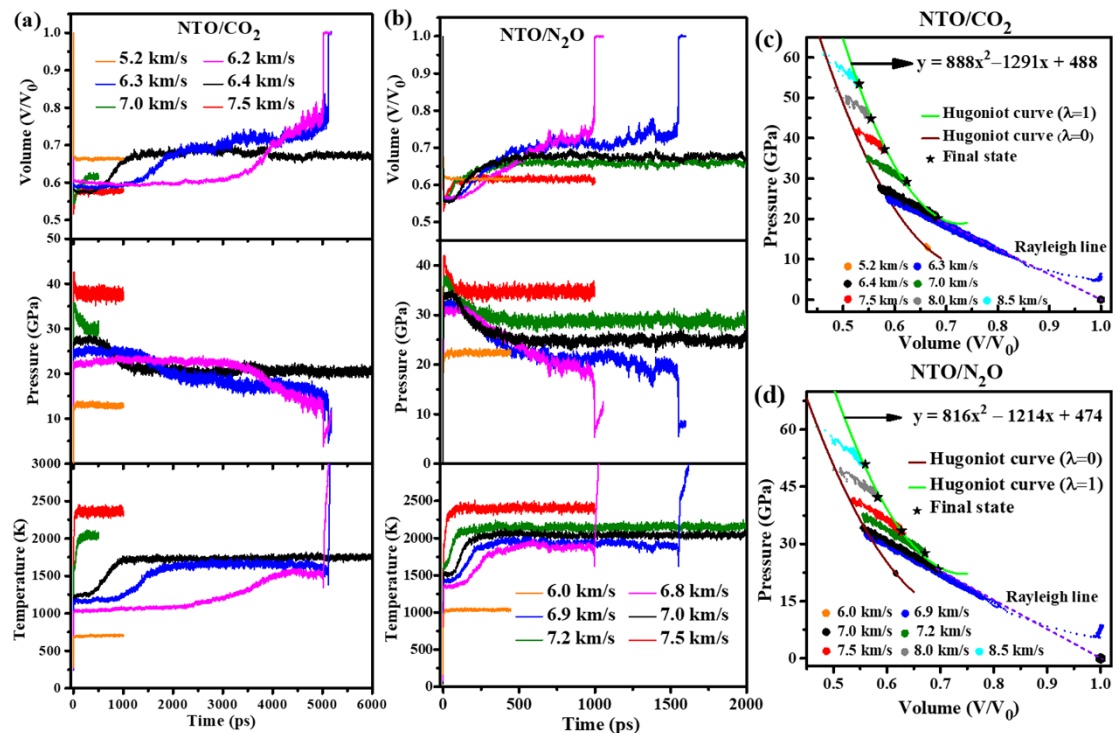


Figure S9. Evolutions of volume, pressure, and temperature behind the shock front for shocks of various speeds propagating through (a) NTO/CO₂ and (b) NTO/N₂O in the y-axis. Simulation trajectories in volume-pressure space for several shock speeds propagating through (c) NTO/CO₂ and (d) NTO/N₂O. In the Hugoniot curves comprising of with volume-pressure space of these two systems, the brown and green solid lines denote the unreacted Hugoniot curve ($\lambda=0$) and the fully reactive Hugoniot curve ($\lambda=1$). The purple dotted line denotes the Rayleigh line for ideal detonation. The black stars denote the final state of shock detonation with different shock velocities.

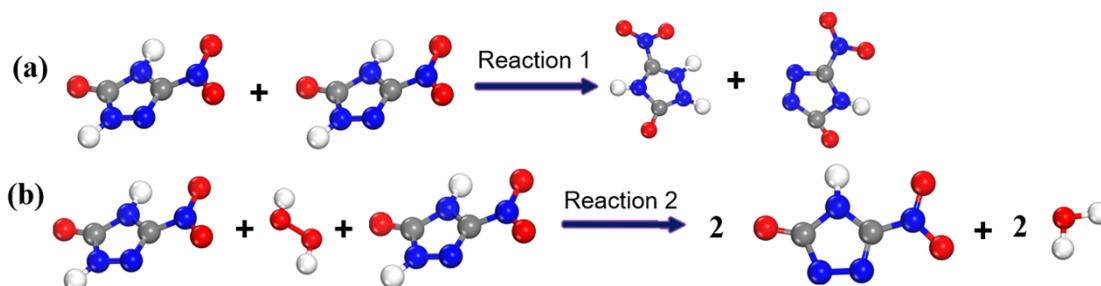


Figure S10. Reaction mechanisms of hydrogen atom transferring to (a) nitrogen atom in the ring during the shock initial reaction stage of NTO crystal. (b) Reaction mechanism of the initial shock reaction in NTO/H₂O₂ crystal. The mechanisms stem from the analysis of MD trajectories during the ideal shock detonation.

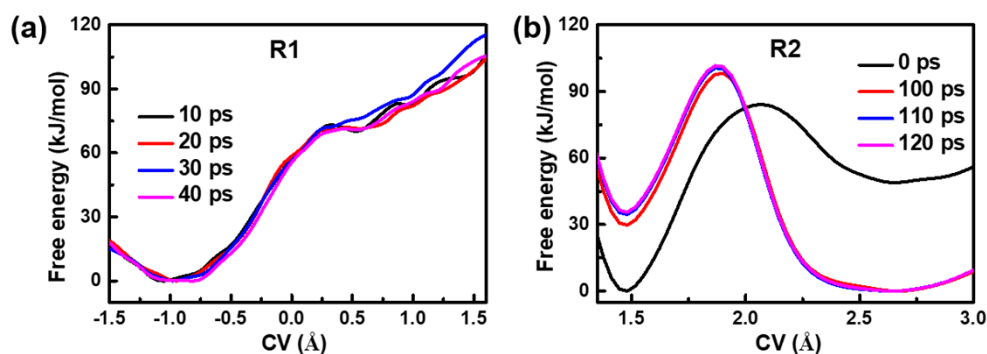


Figure S11. The potential energy landscape of free energy with respect to the collective variables for R1 and R2 at different metadynamics MD simulation times.

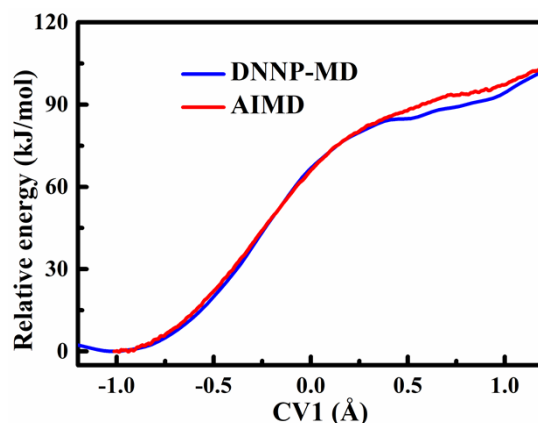


Figure S12. Comparison of calculated potential energy landscapes based on DNNP-MD and AIMD of H atom transferring to N atom within the ring of the NTO crystal. DNNP-MD result was obtained through DNNP-based meta-dynamics and constrained molecular dynamics simulations. AIMD result was derived from Ab-initio molecular dynamics combined with the slow-growth method in VASP.

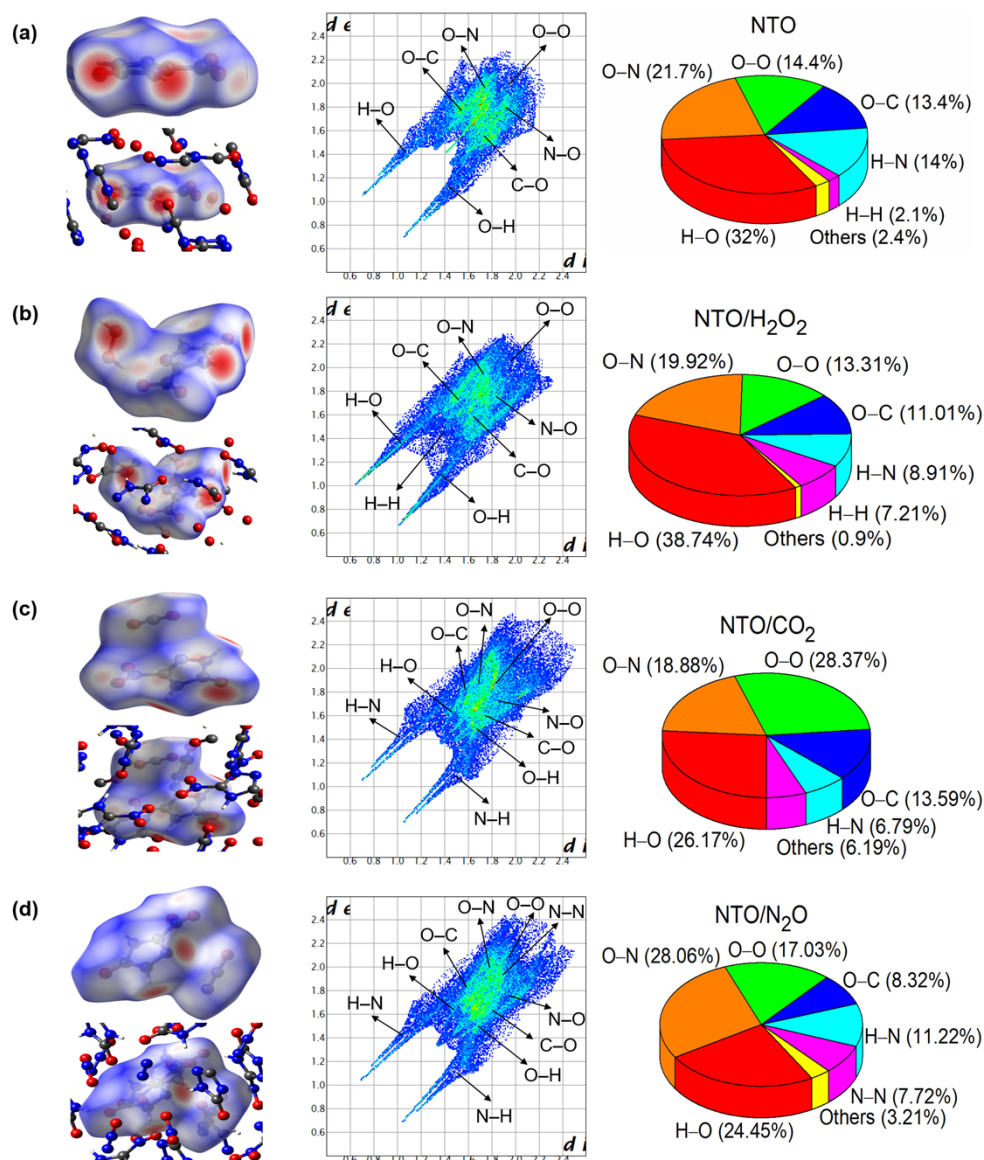


Figure S13. Hirshfeld surface, 2D fingerprint plot, and individual atomic contact percentage contribution to the Hirshfeld surface of (a) NTO crystal, (b) NTO/H₂O₂ crystal, (c) NTO/CO₂ crystal, and (d) NTO/N₂O crystal.